

# Intense AC field driven superlattices with barrier width dimerization

P. H. Rivera<sup>1</sup>, N. Studart<sup>1</sup>, and P. A. Schulz<sup>2</sup>

<sup>1</sup> *Departamento de Física, Universidade Federal de São Carlos  
13564-200, São Carlos, São Paulo, Brazil*

<sup>2</sup> *Instituto de Física ‘Gleb Wataghin’, Universidade Estadual de Campinas  
13083-970 Campinas, São Paulo, Brazil*

(November 14, 2018)

The evolution of two coupled mini-bands, generated by alternating barrier widths dimerization of a superlattice, driven by intense AC fields is investigated. The present model delivers a useful framework for the transition between the analytical high frequency regime and the extreme low frequency limit described by models based on Fukuyama’s *et al.* (Phys. Rev. B **8**, 5579 (1973)) proposal.

PACS 73.20.Dx, 72.20.Ht, 72.15.Rn

The behaviour of semiconductor superlattices (SL)s driven by intense AC fields has been a subject of growing interest in the last few years<sup>1–5</sup>. The theoretical prediction of isolated mini-band collapses<sup>2</sup>, the effect of the AC field on multi-mini-bands and on disordered SLs<sup>6–9</sup> are among the interesting problems studied. Multi-mini-bands systems may be reduced to a simpler one, without loss of the main features, with the suggestion of two almost symmetric mini-bands obtained by a dimerization process on a SL<sup>6</sup>. This dimerized SL can be produced by an alternated sequence of, (1), two quantum wells, or, (2), two barriers, of different widths, keeping the barrier or quantum well (QW) widths constant for (1) and (2), respectively.

These two almost symmetric mini-bands may be strongly coupled by a AC field, whereas remaining isolated from other higher electronic mini-bands. Initially suggested and discussed by Hone and Holthaus<sup>6</sup>, the effect of AC field on dimerized SLs of alternated quantum wells has been systematically studied, either analytically in a high frequency limit<sup>11</sup> or numerically for a wide range of field frequencies<sup>12,13</sup>.

On the other hand, SLs with alternated barriers have been studied for a limited parameter range<sup>14–16</sup>. More general models<sup>5,9,10</sup>, based on Fukuyama’s *et al.* model<sup>19</sup> combine characteristics of both dimerization procedures and show an involved behaviour respect to the field frequency with no clear distinction of different dynamic localization regimes. Our results suggest that these general models should be carefully considered because of the assumptions respect the SL coupling with the field.

In the present work, we show that SLs with alternated barrier widths show a more complex behaviour of the quasi-energy spectra as a function of field intensity compared to SLs with alternating well widths. Our results are based on a heuristic model with its validity investigated by comparison with previous results that take into account explicitly a SL potential profile.

In general there are two different mini-band collapse regimes: isolated mini-band-like and dimer-like collapses. Also, we establish three effective hopping parameter

ranges for the two level systems that show the Stark shift evolution of the SL mini-bands. Due to the variety of parameters involved, only a partial picture of the competition between isolated mini-band behaviour and dynamic localization due to mini-band interactions may be sketched for dimerized SL with alternating barrier widths.

We assume a two-mini-band model in the presence of a strong AC electric field, within a tight-binding framework, emulating the dimerized SL by alternated barriers<sup>6</sup>. A linear chain is considered for this SL, where each single “atomic” *s*-like site orbital is associated to one quantized energy level of a QW. The hopping parameters describe the coupling between the QW levels through the SL barriers. The applied AC fields are parallel to the chain. Hence, our model is described by the Hamiltonian  $H = H_o + H_{int}$ , considering nearest neighbour interaction only:

$$H_o = \sum_{\ell} E_{\ell} |\ell\rangle \langle \ell| + \frac{1}{2} \sum_{\ell} \left\{ \left[ V_1 \frac{(-1)^{\ell} + 1}{2} + V_2 \frac{(-1)^{\ell+1} + 1}{2} \right] |\ell\rangle \langle \ell+1| \right. \\ \left. \left[ V_1 \frac{(-1)^{\ell+1} + 1}{2} + V_2 \frac{(-1)^{\ell} + 1}{2} \right] |\ell+1\rangle \langle \ell| \right\} \quad (1)$$

$$H_{int} = eaF \cos \omega t \sum_{\ell} |\ell\rangle \langle \ell+1| \quad (2)$$

where  $E_{\ell}$  is the *s* orbital energy and  $\ell$  is the index site;  $\omega$  and  $F$  are the AC field frequency and amplitude, respectively.  $a$  is the chain lattice parameter,  $e$  is the electron charge.  $V_1$  e  $V_2$  are hopping parameters that alternate along the chain. The treatment of the time-dependent problem is based on Floquet states  $|\ell, m\rangle$  where  $m$  is the photon index. We follow the procedure first developed by Shirley<sup>17</sup> which consists in the transformation of

the time-dependent Hamiltonian into a time-independent infinite matrix which must be truncated. The matrix elements are:

$$\begin{aligned}
& [(\mathcal{E} - m\hbar\omega - E_\ell)\delta_{\ell'\ell} - \\
& \left[ V_1 \frac{(-1)^\ell + 1}{2} + V_2 \frac{(-1)^{\ell+1} + 1}{2} \right] \delta_{\ell',\ell-1} \\
& \left[ V_1 \frac{(-1)^{\ell+1} + 1}{2} + V_2 \frac{(-1)^\ell + 1}{2} \right] \delta_{\ell',\ell+1}] \times \\
& \delta_{m'm} = F' \ell \delta_{\ell'\ell} (\delta_{m',m-1} + \delta_{m',m+1}) \quad (3)
\end{aligned}$$

where  $F' = \frac{1}{2}eaF$ . The dimension of the matrix is  $L(2M+1)$ , where  $L$  is the number of “atomic” sites, while  $M$  is the maximum photon index. We choose  $M$  in order to satisfy a convergence condition: symmetric spectra relative to the Quasi Brillouin Zones (QBZs) edges<sup>18</sup>. The first QBZ is spanned in the range  $-\hbar\omega/2 \leq \mathcal{E} \leq \hbar\omega/2$ , where  $\mathcal{E}$  represents the eigenvalues of the Floquet matrix, also called as quasi energy.

In what follows, we show the quasi-energy spectra as a function of the electric field intensity, in units of potential drop in through a chain lattice parameter,  $eaF$ . We consider AC external fields with wavelengths that are many times longer than the length of the SL and are linearly polarized along the SL growth direction. We choose to keep the frequency field constant ( $\hbar\omega = 0.5$  meV, corresponding to  $\nu \simeq 0.1$  THz) along the present analysis, while “tuning” the SL parameters (varying the bare mini-band gap  $E_g^0 = 2|V_1 - V_2|$ , while  $E_\ell = 0$  meV fixed for all  $\ell$  sites). This procedure reveals to be very useful for a clear identification of different dynamic localization regimes, for a wide frequency range ( $E_g^0/\hbar\omega \ll 1$  to  $E_g^0/\hbar\omega \gg 1$ ), because of the wide possibilities for independent tight-binding parameters variation. Our calculations consider, in all cases,  $L = 12$  sites and  $M = 80$  photons. The hopping parameters are given for each case, in the corresponding figure.

Depending on the tight-binding parameters, that determine the bare electronic structure, there are qualitatively different behaviours of the dressed states with increasing AC field intensity. First, a distinction is given by the bare mini-band width,  $\Delta^0$ , to field frequency ratio:  $\Delta^0/\hbar\omega < 1$  and  $\Delta^0/\hbar\omega > 1$  situations are illustrated in parts (a) and (b), respectively, for figures (2-6). A second important feature is the mini-band gap to frequency ratio and the figures cover examples across the whole range from  $E_g^0/\hbar\omega \ll 1$  to  $E_g^0/\hbar\omega \gg 1$ . We also will see that the Stark shift drives to resonances between mini-band replicas, leading to an interesting interplay between inter-mini-band and intra-mini-band couplings due to the AC field for  $\Delta^0/\hbar\omega > 1$ . Indeed, in this situation and for low field intensities intra-mini-band coupling is dominant leading to strong anti-crossings at the QBZ edges, as can

be observed in figures (2-6). For high field intensities one could look for effective two level systems in order to describe the Stark shift. One of the main questions to be answered concerns the identification and evolution of isolated mini-band behaviour in SL with barrier width dimerization, having in mind the well width dimerized SLs<sup>12,13</sup>, for which no isolated mini-band behaviour occurs for field intensities above the dynamic breakdown.

In the high frequency regime,  $E_g^0/\hbar\omega \ll 1$  and in  $\Delta^0/\hbar\omega < 1$  situation, the dressed mini-bands resembles the results of an analytical solution given by Bao<sup>16</sup>, reformulated as:

$$\mathcal{E} = \pm \sqrt{(V_1^2 + V_2^2) - 2V_1V_2 \cos(k_z a)} \left| J_0 \left( \frac{eaF}{\hbar\omega} \right) \right| \quad (4)$$

where the mini-band gap, as a function of the field intensity, is defined by  $E_g = 2|V_1 - V_2|J_0(eaF/\hbar\omega)$ . The mini-band width is given by  $\Delta = 2V_1J_0(eaF/\hbar\omega)$ , for  $|V_2| > |V_1|$ ; and  $\Delta = 2V_2J_0(eaF/\hbar\omega)$ , for  $|V_1| > |V_2|$ . On the other hand, in  $\Delta^0/\hbar\omega > 1$  situation, the coupling of the dressed mini-bands is strong for low field intensities and this is not predicted by Eq.(4); only for high field intensities, the evolution of dressed mini-bands is expressed by this. For the regime,  $E_g^0/\hbar\omega < 1$  and in  $\Delta^0/\hbar\omega < 1$  situation, the behaviour based in Eq.(4) also is observed, as can be clearly identified in the numerical results shown in Fig.(1).

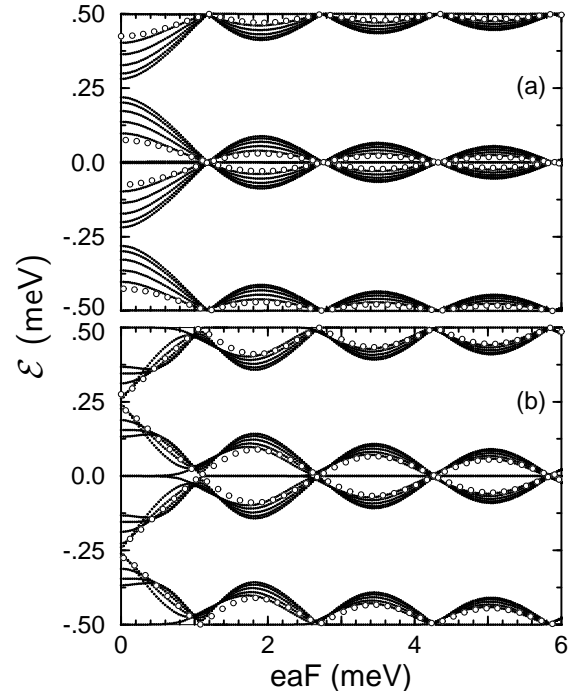


FIG. 1. Quasi energy spectra for dimerized SLs (dots) and dimers (white dots) for  $\Delta^0/\hbar\omega < 1$  in both cases: (a)  $V_1 = 0.15$ ,  $V_2 = 0.075$ ,  $\Delta^0 = 0.15$ ,  $E_g^0 = 0.15$  meV and  $E_g^0/\hbar\omega = 0.3$ ,  $V_{\text{eff}} = 0.075$  meV. (b)  $V_1 = 0.30$ ,  $V_2 = 0.075$ ,  $\Delta^0 = 0.15$ ,  $E_g^0 = 0.45$  meV and  $E_g^0/\hbar\omega = 0.9$ ,  $V_{\text{eff}} = 0.225$  meV.

A further remark concerns to dependence of the surface states relative to the hopping parameters ratio. For  $|V_2| > |V_1|$ , the surface states merge into the mini-bands, while for  $|V_1| > |V_2|$  two “deep” surface states appear, independently from the field intensity, as show in Fig.1.

In this regime, and for  $E_g^0/\hbar\omega \ll 1$ , no signatures of isolated mini-bands are identified; but it should be noticed that a mini-band collapse mechanism is given by the mini-band width modulation according to  $J_0(eaF/\hbar\omega)$ , associated to the mini-gap collapses,  $E_g = 0$ . For larger  $E_g^0$ , isolated mini-band like collapses start to be identified, while the dynamic localization mechanism of interacting mini-band replicas can be described by two level systems with an *effective hopping parameter*,  $V_{\text{eff}}$ . We will call such two level system as an *effective dimer*. The spectra of the *effective dimer* is also shown in Fig.1 (open circles). Here  $V_{\text{eff}} = |V_2 - V_1|$ , as expected from the analytical result for  $E_g$ , derived from Eq.(4).

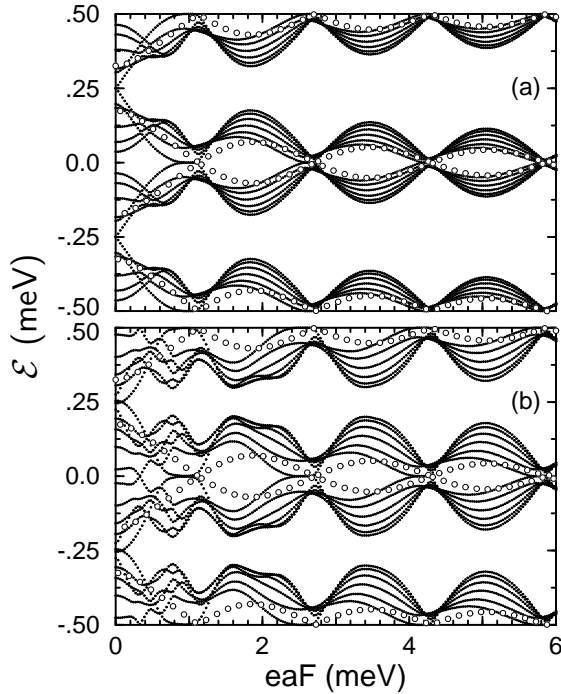


FIG. 2. Quasi energy spectra for dimerized SLs (dots) and dimers (white dots) (a)  $V_1 = 0.15$ ,  $V_2 = 0.325$ ,  $\Delta^0 = 0.30$ ,  $E_g^0 = 0.35$  meV and  $E_g^0/\hbar\omega = 0.7$ ,  $V_{\text{eff}} = 0.175$  meV. (b)  $V_1 = 0.30$  e  $V_2 = 0.475$ ,  $\Delta^0 = 0.60$ ,  $E_g^0 = 0.35$  meV and  $E_g^0/\hbar\omega = 0.7$ ,  $V_{\text{eff}} = 0.175$  meV.

Fig.2 show quasi energy spectra for SLs with  $E_g^0$  and  $\Delta^0$  of the same order of those in Fig.1. Nevertheless, the spectra are quite different, markedly at low field intensities. The important difference is related to the role of the surface states, merged in the mini-bands in the spectra of Fig.2. The Stark shift of the mini-bands, however, is still well described by the same class of *effective dimer* for high field intensities. Although derived from a high frequency limit, the *effective dimer* describes the Stark

shift and consequent crossing and anti-crossings of the mini-bands for the relatively wide  $E_g^0/\hbar\omega \leq 1$  range.

For lower frequencies, i.e.,  $E_g^0/\hbar\omega \sim 1$ , the modulation of the mini-band width and the mini-band gap do not resemble anymore the simple analytical model of Eq.(4). In fact, dimer-like dynamic localization occurs for  $1 < E_g^0/\hbar\omega < 2$ , irrespective to the  $\Delta^0/\hbar\omega$  ratio. But, the Stark shift can not be described by an *effective dimer* for a wide field intensity range. The resonances of mini-band replicas induced by Stark shift may be fitted with an *effective hopping parameter*, which evolves from  $|V_2 - V_1|$  to  $V_2$ . An example of this evolution is show in Fig.3, where spectra of corresponding two level systems are not shown. Here, quasi energy spectra for SLs with  $1 < E_g^0/\hbar\omega < 2$  and  $\Delta^0/\hbar\omega < 1$ , Fig.3.a, and  $\Delta^0/\hbar\omega > 1$ , Fig.3.b, are depicted. For this frequency range signatures of isolated-like mini-band collapses are already seen, although such behaviour becomes clearer for even lower frequencies as will be seen below.

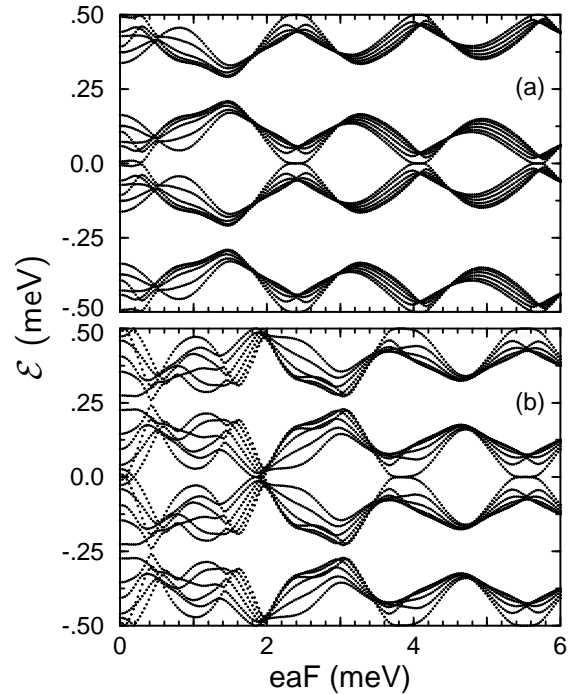


FIG. 3. Quasi energy spectra for dimerized SLs (dots) and dimers (white dots) (a)  $V_1 = 0.15$ ,  $V_2 = 0.525$ ,  $\Delta^0 = 0.30$ ,  $E_g^0 = 0.75$  meV and  $E_g^0/\hbar\omega = 1.5$ ,  $V_{\text{eff}} = |V_2 - V_1| \rightarrow V_2$ . (b)  $V_1 = 0.30$  e  $V_2 = 0.75$ ,  $\Delta^0 = 0.60$ ,  $E_g^0 = 0.90$  meV and  $E_g^0/\hbar\omega = 1.8$ ,  $V_{\text{eff}} = |V_2 - V_1| \rightarrow V_2$ .

Fig.3.a delivers a further important information concerning the validity of our model, when compared to Fig.3 from reference<sup>20</sup>, where the energy gap at zero field is 1.7 meV and the photon energy 1 meV: both spectra are similar and belongs to the same parameter range. This comparison confirms that our heuristic model describes very well the main features of the spectra of a

dimerized SL driven by intense AC fields.

The description of the mini-bands Stark shift with the consequent induced crossings and anti-crossing by an *effective dimer* becomes feasible again for even lower frequencies, i.e.,  $2 \leq E_g^0/\hbar\omega$ , but now the effective dimer is given by  $V_{\text{eff}} = V_2$ . Two examples of this situation are illustrated in Fig.4, where the multi-photon resonances are well described by resonances in the effective dimer spectra. Concerning the comparison of SLs to the corresponding two level systems, the dimer-like collapses of these mini-bands are observed and associated to the resonances of dimers with *effective hopping parameters* given by:

$$V_{\text{eff}} = \begin{cases} |V_2 - V_1| & \text{for } E_g^0/\hbar\omega \leq 1 \\ |V_2 - V_1| \rightarrow V_2 & \text{for } 1 < E_g^0/\hbar\omega < 2 \\ V_2 & \text{for } 2 \leq E_g^0/\hbar\omega \end{cases} \quad (5)$$

The isolated mini-band behaviour with the associated dynamic localization for field intensities corresponding to zeros of  $J_0(e2aF/\hbar\omega)$  can be clearly identified in the spectrum shown in Fig.4(a). The mini-band collapse for  $eaF \approx 0.6$  meV corresponds to the first root of the zero order Bessel function taking into account the period of the SL,  $2a$ . Signatures of further isolated-like mini-band collapses for higher field intensities are barely identified in this case. However, increasing further  $E_g^0/\hbar\omega$ , clear isolated mini-band behaviour may be seen up to very high field intensities, irrespective to the presence of mini-band resonances, as can be seen in Figs.5 and 6.

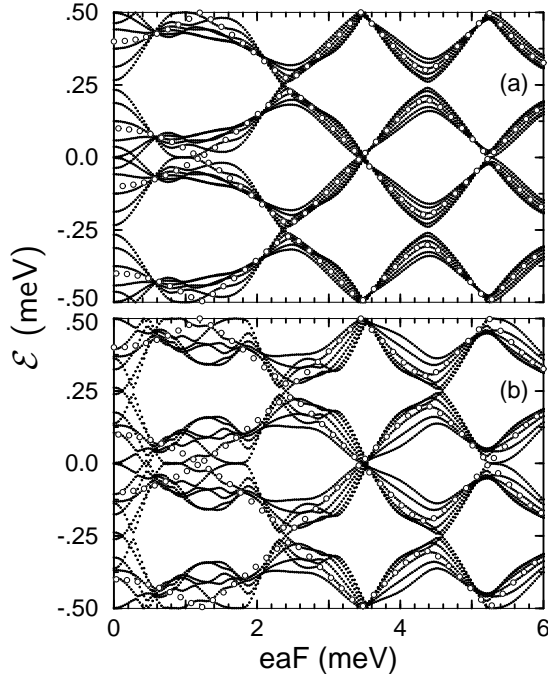


FIG. 4. Quasi energy spectra for dimerized SLs (dots) and dimers (white dots) (a)  $V_1 = 0.15$ ,  $V_2 = 0.90$ ,  $\Delta^0 = 0.30$ ,  $E_g^0 = 1.50$  meV and  $E_g^0/\hbar\omega = 3.0$ ,  $V_{\text{eff}} = 0.90$  meV. (b)  $V_1 = 0.30$  e  $V_2 = 0.90$ ,  $\Delta^0 = 0.60$ ,  $E_g^0 = 1.20$  meV and  $E_g^0/\hbar\omega = 2.40$ ,  $V_{\text{eff}} = 0.90$  meV.

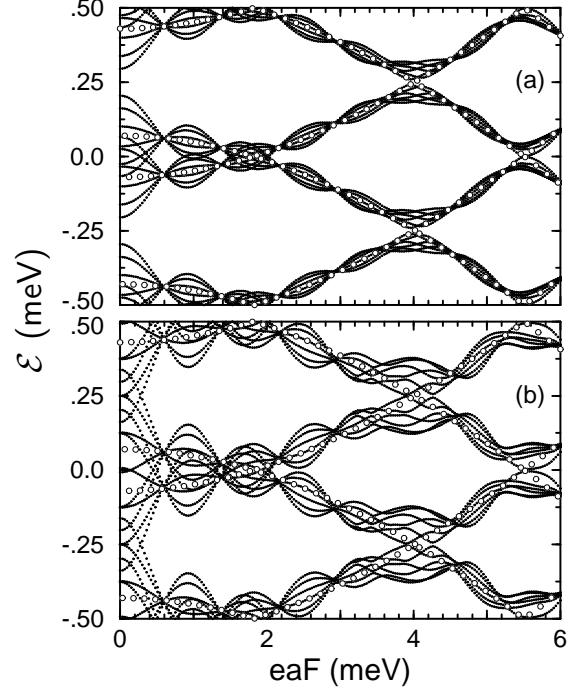


FIG. 5. Quasi energy spectra for dimerized SLs (dots) and dimers (white dots) (a)  $V_1 = 0.15$ ,  $V_2 = 2.93$ ,  $\Delta^0 = 0.30$ ,  $E_g^0 = 5.56$  meV and  $E_g^0/\hbar\omega = 11.12$ ,  $V_{\text{eff}} = 2.93$  meV. (b)  $V_1 = 0.30$  e  $V_2 = 2.93$ ,  $\Delta^0 = 0.60$ ,  $E_g^0 = 5.26$  meV and  $E_g^0/\hbar\omega = 10.52$ ,  $V_{\text{eff}} = 2.93$  meV.

In the low frequency range, together with a high  $V_2/V_1$  ratio, depicted in Figs.5 and 6, one has the limit of the Stark shift and related mini-band resonances well described by a system of two levels with an interaction described by the hopping parameter  $V_2$ . Less intense inter-dimer interaction, essentially described by the hopping parameter  $V_1$ , leads to a relatively small mini-band dispersion. In this limit the mini-band dispersion is not affected by mini-band interactions except for field intensities very close to multi-photon resonances. Nevertheless, strong mini-band interaction can be seen for  $eaF \approx 4$  meV for a relatively wide mini-band case, Fig.5. Important, however, is that the isolated mini-band behaviour is recovered by further increasing the field intensity up to values for which a new multi-photon resonance occur at  $eaF \approx 5.5$  meV. Such recovering of isolated mini-band behaviour for field intensities beyond a strong mini-band interaction does not occur with SL dimerized by alternating well widths<sup>13</sup>. The main difference lies on the fact that in the alternating well width case  $E_g^0$  is mainly determined by the quantum well states. For field intensities that exceed the quantum well levels separation in energy a not recoverable breakdown occurs. In the present case of alternating barrier width, the bare mini-gap is given by the difference between hopping parameters and the mini-band dispersion determined by the smaller one. Hence,

the mini-band dispersion may be seen as a perturbation of the effective dimer and the breakdown is recoverable with further increasing of the field intensity.

For  $E_g^0/\hbar\omega \gg 1$ , the interaction between mini-bands is negligible for the field intensities shown in Fig.6. Actually, the avoided crossings are not resolved in the spectra, because the associated multi-photon resonances are for a very high photon number. Therefore, no dynamic breakdown is observed and the isolated mini-band character is preserved beyond such mini-band interactions.

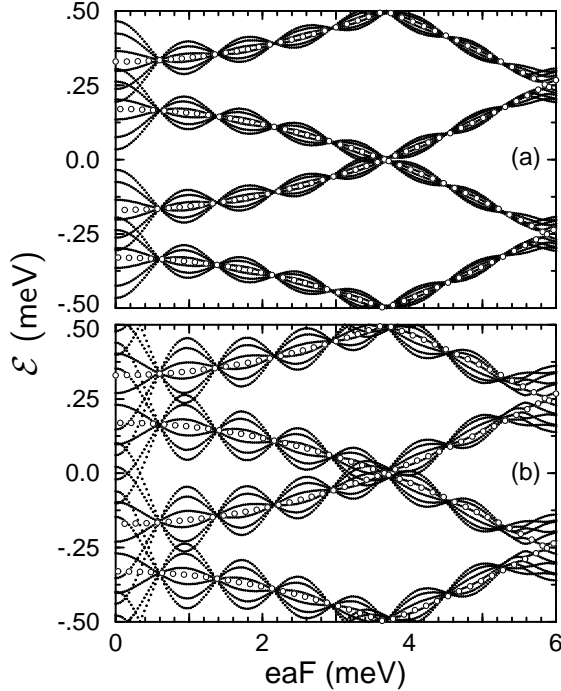


FIG. 6. Quasi energy spectra for dimerized SLs (dots) and dimers (white dots) (a)  $V_1 = 0.15$ ,  $V_2 = 4.83$ ,  $\Delta^0 = 0.30$ ,  $E_g^0 = 9.36$  meV and  $E_g^0/\hbar\omega = 18.72$ ,  $V_{\text{eff}} = 0.90$  meV. (b)  $V_1 = 0.30$  e  $V_2 = 4.83$ ,  $\Delta^0 = 0.60$ ,  $E_g^0 = 9.06$  meV and  $E_g^0/\hbar\omega = 18.12$ ,  $V_{\text{eff}} = 0.9$  meV.

In conclusion, we propose a tight-binding model for SLs dimerized by alternating barrier widths. Our model, although heuristic, takes into account explicitly the barrier widths alternation in the proper hopping parameters. The heuristic character is only related to the construction of the bare SL. Within this framework, no further assumptions on the coupling of the SL with the AC field are made. The numerical results show that the model is appropriate irrespective to the  $E_g^0/\hbar\omega$  ratio. One of the main findings of the present work is the inspection of the validity range of the analytical high frequency limit, as well of the models based on Fukuyama *et al.*<sup>19</sup>, appropriate only for  $E_g^0/\hbar\omega \gg 1$  and do not reproduce the

high frequency limit. Furthermore, the present work elucidates the important differences between the dimerization by alternating barrier widths and by alternating well widths<sup>13</sup>. For dimerization by alternating well widths, a clear breakdown is identified, while for the situation illustrated in Fig.6, alternating very thin with relatively thick barriers, the isolated mini-band behaviour may be periodically recovered as a function of increasing field intensity.

The authors acknowledge CAPES, FAPESP and CNPq for financial support.

- 
- <sup>1</sup> D. H. Dunlap and V. M. Kenkre, *Phys. Rev. B* **34**, 3625 (1986)
  - <sup>2</sup> M. Holthaus, *Phys. Rev. Lett.* **69**, 351 (1992)
  - <sup>3</sup> P. S. S. Guimarães, B. J. Keay, J. P. Kaminski, S. J. Allen, P. F. Hopkins, A. C. Gossard, L. T. Florez, and J. P. Harbison, *Phys. Rev. Lett.* **70**, 3792 (1993)
  - <sup>4</sup> B.J.Keay, S. Zeuner, S. J. Allen, K. D. Maranowski, A. C. Gossard, U. Bhattacharya, and M. J. W. Rodwell, *Phys. Rev. Lett.* **75**, 4102 (1995)
  - <sup>5</sup> Jon Rotvig, Antti-Peka Jauho, and Henrik Smith, *Phys. Rev. Lett.* **74**, 1831 (1995)
  - <sup>6</sup> Daniel W. Hone and Martin Holthaus, *Phys. Rev. B* **48**, 15123 (1993)
  - <sup>7</sup> M. Holthaus, G. H. Ristow, and D. W. Hone, *Europhys. Lett.* **32**, 241 (1995)
  - <sup>8</sup> Martin Holthaus and Gerard H. Ristow, *Phys. Rev. Lett.* **75**, 3914 (1995)
  - <sup>9</sup> Klaus Drese and Martin Holthaus, *J. Phys.: Condens. Matter* **8**, 1193 (1996)
  - <sup>10</sup> M. Holthaus and D. Hone, *Phil. Mag.* **74**, 105 (1996)
  - <sup>11</sup> Xian-Geng Zhao, *J. Phys.: Condens. Matter* **9**, L385 (1997)
  - <sup>12</sup> P. H. Rivera and P. A. Schulz, *Proc. 24<sup>th</sup> Int. Conf. on Phys. of Semicond.*, Jerusalem, Israel; Ed. David Gershoni, World Scientific, Singapore (1998)
  - <sup>13</sup> P. H. Rivera and P. A. Schulz, *cond-mat/9908031*, Aug (1999)
  - <sup>14</sup> Xian-Geng Zhao e Qian Niu; *Phys. Lett. A* **222**, 435 (1996)
  - <sup>15</sup> Xian-Geng Zhao, G. A. Georgakis e Qian Niu; *Phys. Rev. B* **54**, R5235 (1996)
  - <sup>16</sup> Shu-Qing Bao, Xian-Geng Zhao, Xin-Wei Zhang, and Wei-Xian Yan, *Phys. Lett. A* **240**, 185 (1998)
  - <sup>17</sup> Jon H. Shirley, *Phys. Rev.* **138**, B979 (1965)
  - <sup>18</sup> M. Holthaus, *Z. Phys. B* **89**, 251 (1992)
  - <sup>19</sup> H. Fukuyama, R. A. Bari, and H. C. Fogedby, *Phys. Rev. B* **8**, 5579 (1973)
  - <sup>20</sup> Martin Holthaus and Daniel W. Hone, *Phys. Rev. B* **49**, 16605 (1994)